Electronic Supporting Information

Boosting the oxygen reduction activity of three-dimensional network Co-N-C electrocatalyst *via* space-confined control of nitrogen-doping efficiency and molecular-level coordination effect

Chaozhong Guo [a†*], Yanrong Li [b†], Wenli Liao [a†], Yao Liu [a†], Zhongbin Li [a], Lingtao Sun [a], Changguo Chen [c], Jin Zhang [a,b], Yujun Si [d**], Lu Li [a***]

[a] Research Institute for New Materials Technology, School of Materials and Chemical Engineering, Engineering Research Center of New Energy Storage Devices and Applications, Chongqing University of Arts and Sciences, Chongqing 402160, China

[b] College of Materials Science and Engineering, College of Chemistry and Chemical Engineering, Chongqing University of Technology, Chongqing 400054, China

[c] College of Chemistry and Chemical Engineering, Chongqing University, Chongqing 400044, Shapingba, China

[d] College of Chemistry and Environmental Engineering, Sichuan University of Science and Engineering, Zigong, 643000, China

[†]These authors equally contributed to this work, and they are considered as the co-first author.

*Corresponding authors. E-mail: guochaozhong1987@163.com (C. Guo); syj08448@163.com (Y. Si); lilu25977220@163.com (L. Li)

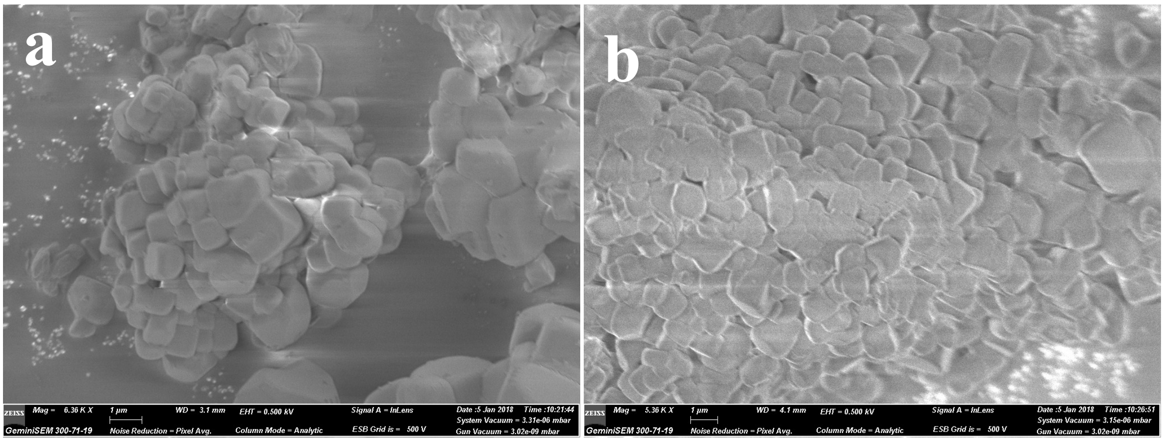

Fig. S1. The SEM images (a,b) of the Co-TPTZ@3D-NaCl precursor.

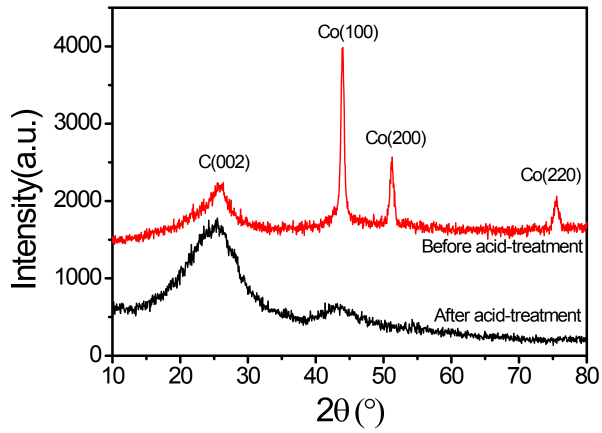

Fig. S2. XRD pattern of 3D-Co-N-C before and after acid-treatment process.

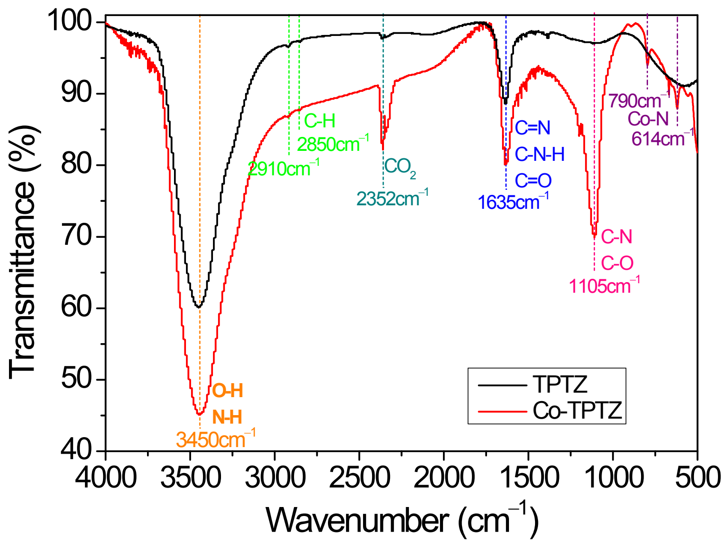

Fig. S3. Fourier transform infrared spectrometer (FT-IR) spectra of TPTZ and Co-TPTZ.

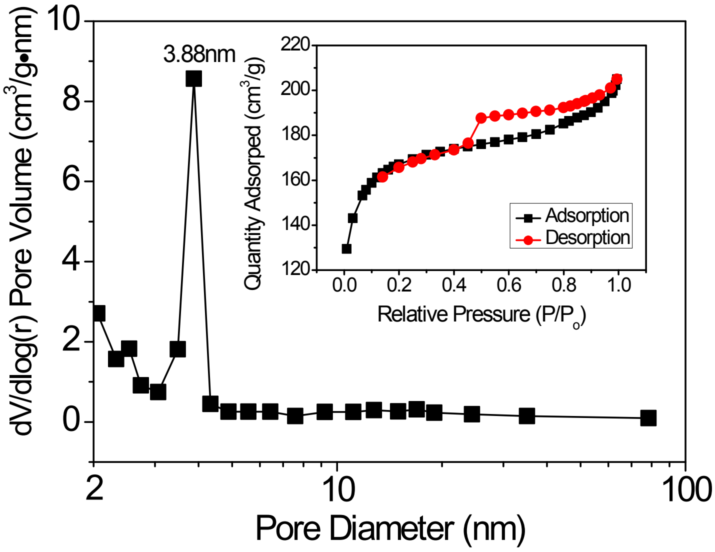

Fig. S4. The pore-size distribution of Co-N-C; Inset is the N_2 adsorption-desorption isotherms.

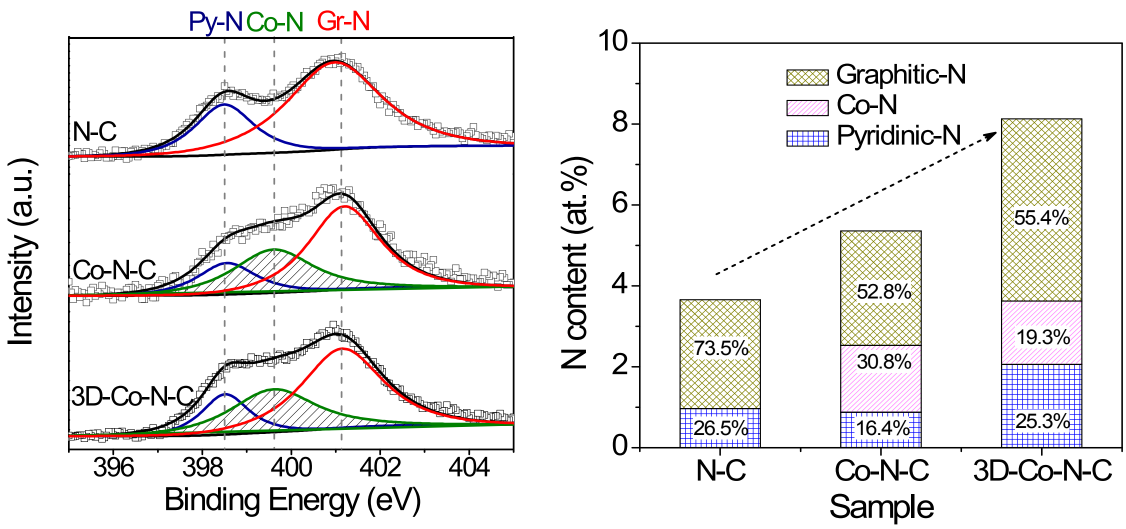

Fig. S5. (a) The comparison of N1s XPS spectra of N-C, Co-N-C and 3D-Co-N-C. (b) The content distribution of vaious nitrogen-rich groups in the prepared catalysts.

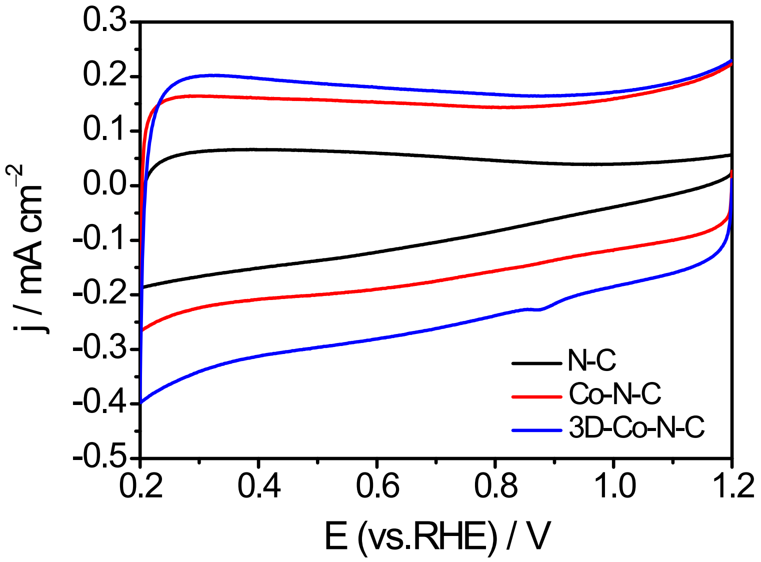

Fig. S6. CV curves of N-C, Co-N-C and 3D-Co-N-C in N_2-saturated 0.1 M KOH solution.

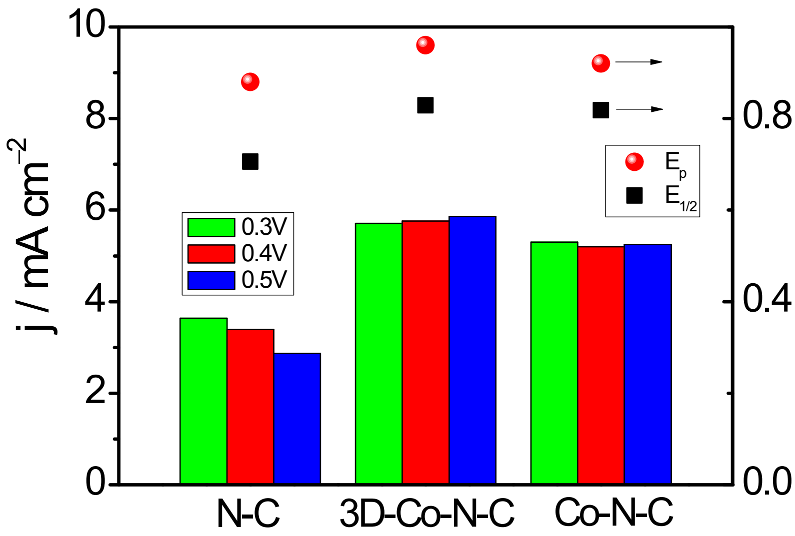

Fig. S7. The electrocatalytic activity comparison among N-C, Co-N-C and 3D-Co-N-C in terms of ORR peak potential, ORR half-wave potential and limited current density at given potentials.

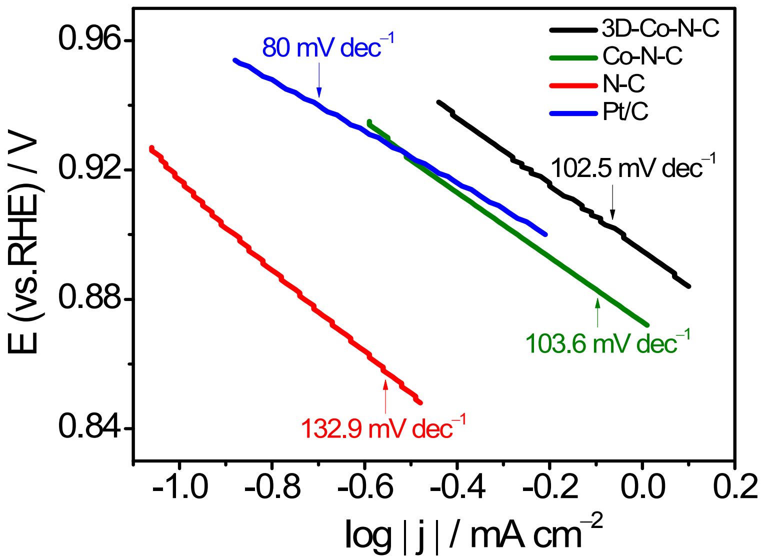

Fig. S8. The Tafel curve of prepared catalysts in the range of 0.84-0.96 V.

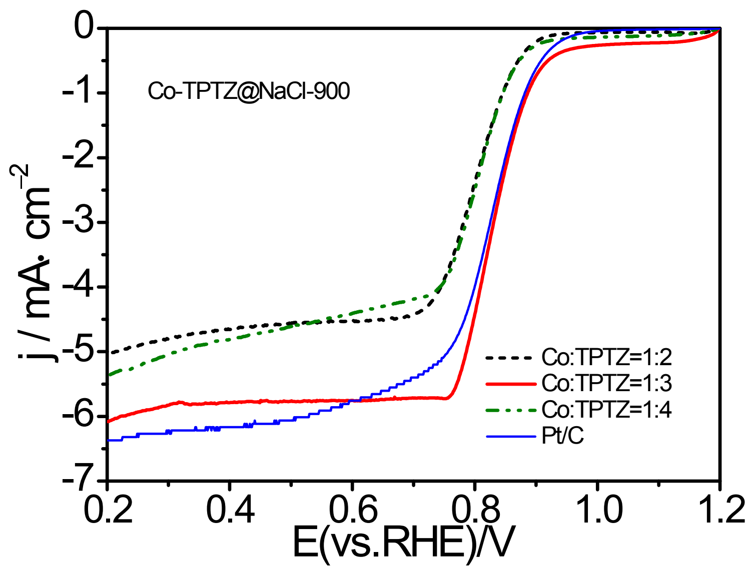

Fig. S9. LSV curves for ORR of 3D-Co-N-C catalysts with different ratios of cobalt ions coordinated with TPTZ ligand.

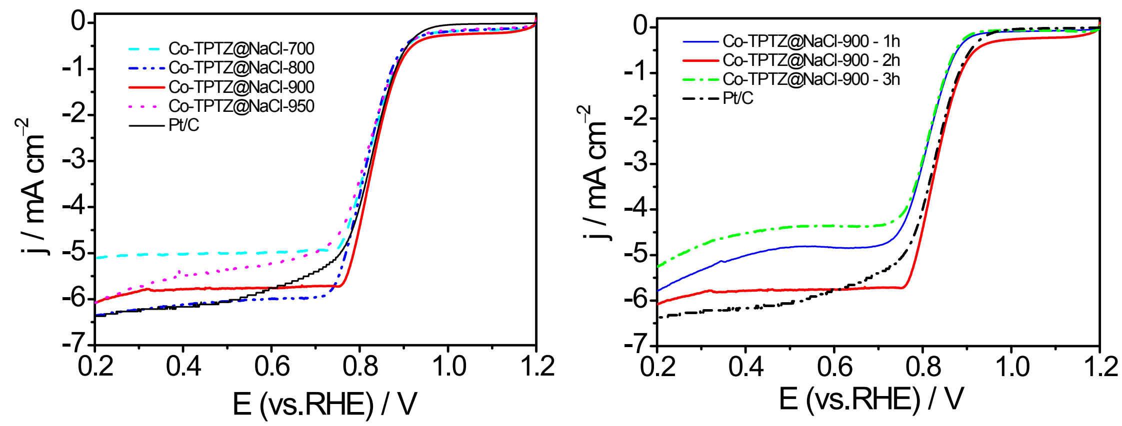

Fig. S10. LSV curves for ORR of 3D-Co-N-C catalysts obtained from different heat-treatment temperatures (a) and heat-treatment times (b).

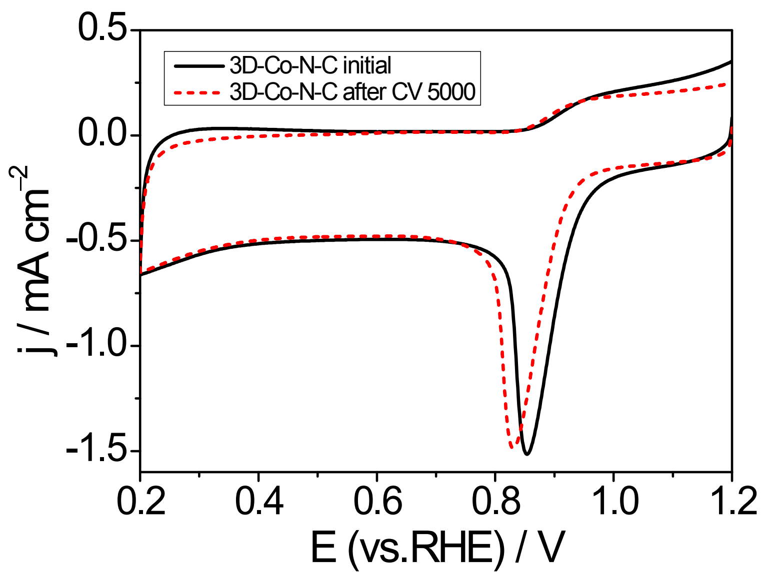

Fig. S11. CV curves for ORR of 3D-Co-N-C before and after CV for 5000 cycles in O_2-saturated 0.1 M KOH electrolyte.

Table S1. The ORR activity data for 3D-Co-N-C and other similar carbon-based electrocatalysts.

Samples	$E_{\mathbf{ORR}}$	$\mathbf{E_{1/2}}$	**n**	$\mathbf{J_d}$	**References**
Co-NC(900)	0.85V (*vs*.RHE)	0.80 V *vs*.RHE	3.9	5.5 mA cm^{-2} @ + 0.65 V *vs*.RHE	[36]
FeN/C-PANI	0.99V (*vs*.RHE)	0.85 V *vs*.RHE	4.0	5.3 mA cm^{-2} @ + 0.65 V *vs*.RHE	[37]
Co/N/C-A	0 V *vs*.Hg/HgO	---	4.1	4.2 mA cm^{-2} @ –0.4 V *vs*. Hg/HgO	[38]
CoN/C-600	0.91 V (*vs*.RHE)	0.85 V *vs*.RHE	3.8	5.7 mA cm^{-2} @ + 0.55 V *vs*.RHE	[39]
BP350C1000	0.90 V (*vs*.RHE)	0.78 V *vs*.RHE	3.5	1.0 mA cm^{-2} @ + 0.65 V *vs*.RHE	[40]
N-Graphene (900)	0.31 V (*vs*.SHE)	0.35 V *vs*.SHE	3.6	3.0 mA cm^{-2} @ –1.0 V *vs*.SHE	[41]
GO flakes	–210 mV (*vs*.Ag/AgCl)	---	1.9	3.7 mA cm^{-2} @ –1.0 V *vs*.Ag/AgCl	[42]
Fe-PANI@GD-900	1.05 V (*vs*.RHE)	0.82 V *vs*.RHE	4.0	4.5 mA cm^{-2} @ 0.5 V *vs*. RHE	[43]
750-8N-CNO	0.05 V (vs.Ag/AgCl)	---	4.1	4.0 mA cm^{-2} @ –0.60 *vs*. Ag/AgCl	[44]
Co-Nx@CNF700	0.941 V (*vs*.RHE)	0.814 V *vs*. RHE	3.9	5.5 mA cm^{-2} @ 0.65 *vs*. RHE	[45]
ZnN_x/BP	0 V (vs.SCE)	-175 mV *vs*. SCE	4.0	6.0 mV cm^{-2} @ 0.60 *vs*. SCE	[46]
Co_9S_8/N,S-CNS	0.90 V (vs.RHE)	0.80 V vs.RHE	3.8	4.5 mV cm^{-2} @ 0.60 *vs*. RHE	[47]
N-HCNs	0.931 V (vs.RHE)	0.84 V vs.RHE	3.9	5.5 mA cm^{-2} @ 0.65 *vs*. RHE	[48]
3D-Co-N-C	1.0 V (*vs*.RHE)	0.83 V *vs*. RHE	3.8	5.9 mA cm^{-2} @ 0.65 *vs*. RHE	This work

Table S2. The BET surface area (S_{BET}) and total nitrogen content of N–doped carbon catalysts and their corresponding ORR activities.

Samples	E_{ORR} (*vs.*RHE)	$E_{1/2}$ (*vs.* RHE)	j_d	N content (at. %)	S_{BET} ($m^2\ g^{-1}$)	References
Co–N_x@CNF700	0.94 V	0.81 V	5.5 mA cm^{-2} @ 0.65 *vs.* RHE	1.96	452.44	[45]
N'N–GDY	0.98 V	0.84 V	4.37 mA cm^{-2} @ 0.65 *vs.* RHE	3.67	1154	[49]
NGR–900	0.90 V	0.80 V	2.9 mV cm^{-2} @ 0.60 *vs.* RHE	2.74	771	[50]
ANPC–3	0.81 V	0.75 V	5.09 mA cm^{-2} @ 0.8 V vs. RHE	2.77	1749	[51]
Fe/N/APC–900	0.96 V	0.88 V	6.3 mA cm^{-2} @ 0.60 *vs.* RHE	1.87	1083	[52]
NCF–900	1.05 V	0.89 V	8.66 mA cm^{-2} @ 0.60 *vs.* RHE	1.96	1547	[53]
CNFe	0.99 V	0.90 V	6.01 mA cm^{-2} @ 0.60 *vs.* RHE	3.20	1141	[54]
NGS4–900	0.98 V	0.85 V	5.98 mA cm^{-2} @ 0.60 *vs.* RHE	2.0	137	[55]
CSs–20h–900	0.98 V	0.84 V	4.2 mA cm^{-2} @ 0.60 *vs.* RHE	---	756	[56]
NSMC–900	0.98 V	0.85 V	5.5 mA cm–2 @ 0.50 *vs.* RHE	2.19	499	[57]
3D–Co–N–C	1.00 V	0.83 V	5.9 mA cm^{-2} @ 0.65 *vs.* RHE	8.13	638	This work

References

36. C. Guo, Y. Wu, Z. Li, W. Liao, L. Sun, C. Wang, B. Wen, Y. Li and C. Chen, Nanoscale Res. Lett., 2017, 12, 144.
37. C. Guo, B. Wen, W. Liao, Z. Li, L. Sun, C. Wang, Y. Wu, J. Chen, Y. Nie, J. Liao and C. Chen, *J. Alloys Comp*. **2016**, 686, 874.
38. Z. Ma, C. Guo , Y. Yin, Y. Zhang, H. Wu and C. Chen, *Electrochim. Acta* **2015**, 160, 357.
39. S. Chao and M. Jiang, *Int. J. Hydrogen Energ.* **2016**, 41,12995.
40. C. Guo, C. Chen and Z. Luo, J. Power Sources **2014**, 245, 841.
41. D. Geng, Y. Chen, Y. Chen, Y. Li, R. Li, X. Sun, S. Ye and S. Knights, *Energy Environ. Sci.* **2011**, 4, 760.
42. J. Liu, H. Yang, S. Zhen, C. Poh, A. Chaurasia, J. Luo, X. Wu, E. Yeow, N. Sahoo, J. Lin and Z. Shen, *RSC adv.* **2013**, 3, 11745.
43. Y. Li, C. Guo, J. Li, W. Liao, Z. Li, J. Zhang and C. Chen, *Carbon* **2017**, 119, 201–210.
44. K. Chatterjee, M. Ashokkumar, H. Gullapalli, Y. Gong, R. Vajtai, P. Thanikaivelan and P. M. Ajayan, *Carbon* **2018**, 130, 645–651.
45. K. R. Yoon, J. Choi, S.–H. Cho, J.–W. Jung, C. Kim, J. Y. Cheong and I.–D. Kim, *J. Power Sources* **2018**, 380, 174–184.
46. P. Song, M. Luo, X. Liu, W. Xing, W. Xu, Z. Jiang and L. Gu, *Adv. Funct. Mater.* **2017**, 1700802.
47. C. Wu, Y. Zhang, D. Dong, H. Xie and J. Li, *Nanoscale* **2017**, 9, 12432–12440.
48. J. Zhu, H. Zhou, C. Zhang, J. Zhang and S. Mu, *Nanoscale* **2017**, 9, 13257–13263.
49. Q. Lv, W. Si, Z. Yang, N. Wang, Z. Tu, Y. Yi, C. Huang, L. Jiang, M. Zhang, J. He and Y. Long, *ACS Appl. Mater. Interfaces* **2017**, 9, 29744–29752.
50. X. Bo, C. Han, Y. Zhang and L. Guo, *ACS Appl. Mater. Interfaces* **2014**, 6, 3023–3030.
51. G. Lin, R. Ma, Y. Zhou, Q. Liu, X. Dong and J. Wang, *Electrochimica Acta* **2018**,261, 49-57.

52. J, Xu, C. Wu, Q. Yu, Y. Zhao, X. Li and L. Guan, *ACS Sustain. Chem. Eng.* **2018**, 6, 551−560.

53. X. Yang, K. Li, D. Cheng, W. Pang, J. Lv, X. Chen, H. Zang, X. Wu, H. Tan, Y. Wang and Y. Li, *J. Mater. Chem. A* **2018**, 6, 7762–7769.

54. W. Li, W. Ding, J. Jiang, Q. He, S. Tao, W. Wang, J. Li and Z. Wei, *J. Mater. Chem. A* **2018**, 6 , 878–883

55. Q. Xiang, Y. Liu, X. Zou, B. Hu, Y. Qiang, D. Yu, W. Yin and C. Chen, *ACS Appl. Mater. Interfaces* **2018**, 10, 10842−10850.

56. Q. Xiang, W. Yin, Y. Liu, D. Yu, X. Wang, S. Li and C. Chen, *J. Mater. Chem. A* **2017**, 5, 24314–24320.

57. A.D. Tan, K. Wan,. Y.-F. Wang, Z.-Y. Fu and Z.-X. Liang, *Catal. Sci. Technol.* **2018**, 8, 335–343.